Journal of Supramolecular Structure 4:449 (409)–465 (425) (1976)

CONJUGATED POLYENE FATTY ACIDS AS FLUORESCENT MEMBRANE PROBES: Model System Studies

Larry A. Sklar, and Bruce S. Hudson

Department of Chemistry, Stanford University, Stanford, California

Robert D. Simoni

Department of Biological Sciences, Stanford University, Stanford, California

The use of conjugated polyene fatty acids as probes of membrane structure is examined. α- and β-parinaric acid (cis, trans, trans, cis- and all trans-9,11, 13, 15-octadecatetraenoic acid) and synthetic lecithins containing an α-parinaric acid chai in position 2 have been prepared, and their absorption and fluorescence properties have been determined. Their absorption spectra are at sufficiently long wavelength to be unobscured by cellular chromophores such as nucleotides and aromatic amin acids. Parinaric acid absorption does, however, overlap tryptophan emission which allows fluorescence energy transfer.

Potential uses of these fluorescent probes are presented with studies on mode systems with known physical properties. Dipalmitoyl phosphatidylcholine exhibits a sharp phase transition 1° wide at $42^{\circ}C$, as monitored by the fluorescence intensit of parinaric acid. The magnitude of the transition is independent of probe concentration, but the width of the transition and hysteresis are dependent upon such factors as the probe concentration and whether or not sonication is used in sample preparation. Using both fluorescence and absorption properties of the probe, we show that the addition of cholesterol to the dispersion broadens and decreases the magnitude of the transition. These results are interpreted in terms of a change in the polarizability of the acyl chains of a lipid bilayer as the bilayer undergoes a thermal transition.

Lipid-protein interactions are studied by the binding of α-parinaric acid to bovine serum albumin. Fluorescence enhancement, absorption spectral shifts, and quenching of tryptophan fluorescence are observed when α-parinaric acid binds to bovine serum albumin. Calculations based on these measurements are consistent with two binding sites of $K_B \sim 10^8$ (M^{-1}) and three to four binding sites of $K_B \sim 10^6 - 10^7$ (M^{-1}), similar to known values for the binding of other long-chain fatty acids.

Biosynthetic incorporation of β-parinaric acid into the E. coli fatty acid auxotroph 30E βox⁻ has been accomplished and phase transitions in cells and isolated phospholipids are shown.

INTRODUCTION

Fluorescence spectroscopy of molecular probes has provided much insight into the complexities of biological membranes (1–3). The prime advantages of fluorescent probe techniques are their great detection sensitivity, the sensitivity of probes to their environment, and the large number of parameters that can be monitored continuously and on a rapid time scale. These parameters include absorption, excitation, and emission spectra, quantum yield, lifetime, and polarization. Interpretation of data collected in these ways can provide insight into the structure-function relationship of membrane lipids and proteins.

The general use of fluorescent chromophores, however, suffers from several major disadvantages. Molecules such as 1-anilinonaphthalene-8-sulfonate (ANS) and related compounds have been used extensively (1), but yield data that are often difficult to interpret, in part because the location of the probe is uncertain. This difficulty may be minimized by probes such as 12-(9-anthroyl)stearic acid that are derivatives of normal membrane components (2). While probes of this type have somewhat more predictable locations and orientation in model lipid systems and biological membranes, they suffer from the disadvantage of chromophore bulk and the inevitable perturbations of the system that result. Moreover, understanding changes in the spectral properties of such complex substituted aromatic chromophores is difficult.

It is the purpose of this report to extend our initial efforts (4) toward establishing the use of a unique class of fluorescent probes for biological membranes. The chromophoric molecules we have used are polyunsaturated fatty acids in which the double bonds are conjugated. The structure and conformation of these molecules closely resemble those of normally occurring membrane components and one would expect minimal perturbations. Furthermore, the location and orientation of the chromophore relative to the surroundings is predictable. Recent studies of the electronic spectroscopy of linear polyenes (5) can be used to advantage in their application to membrane studies. These molecules as a class, hereafter referred to simply as polyenes, offer wide variability of structure and potential applications. Polyene fatty acids can be prepared with different numbers of double bonds, cis-trans geometrical forms, and overall chain length. We feel that these probes possess the advantages of the fluorescence technique while minimizing the disadvantages.

α-Parinaric acid (9, 11, 13, 15-cis, trans, trans, cis-octadecatetraenoic acid) is one of several naturally occurring linear polyene fatty acids. Among others, α- and β-eleostearic acid (9, 11, 13-cis, trans, trans and 9, 11, 13—all trans octadecatrienoic acid) are available, but their absorption and fluorescence spectra are in the same regions as those of tryptophan, which is a considerable obstacle to their use as probes in biological systems. Although the absorption spectra of α and β (all trans) parinaric acid have been reported (6–8), no systematic studies of their spectral properties have been undertaken, and, to our knowledge, there are no previous reports by other groups of the fluorescence properties of these molecules. These tetraenes and molecules with longer conjugated regions are well suited spectrally as probes. The diphenylpolyenes (9) and the polyene antibiotics (10) have been previously used as probes in membrane systems.

This paper reports the use of the two isomers of parinaric acid, and some synthetic derivatives of phosphatidyl cholines bearing a parinaric acid esterified to position 2, in a variety of model system studies and includes a discussion of the nature of the environmental parameters measured by the probe.

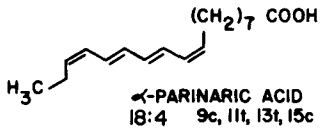

α-PARINARIC ACID
18:4 9c, 11t, 13t, 15c

β-PARINARIC ACID
18:4 9t, 11t, 13t, 15t

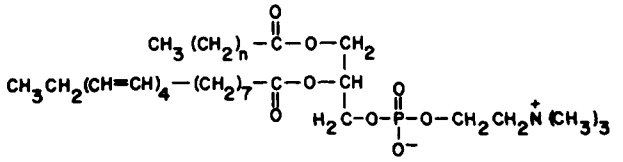

2-PARINAROYL PHOSPHATIDYL CHOLINE

MATERIALS AND METHODS

Preparation of Parinaric Acid and Phospholipid Derivatives

Descriptions of the procedures have appeared in a preliminary report (4). The α and β isomers of parinaric acid can be prepared 99% pure.

Lipid Dispersions

Chloroform solutions of the appropriate lipid, containing 0.25 mg unless otherwise specified, were dried under vacuum in a small round-bottom flask. Dispersion in 5 ml 0.01 M phosphate buffer, pH 7.5, was accomplished by vortexing the sample under argon, above the transition temperature, for 30 sec. In general, the scattering contribution to optical density was less than 0.10 at 320 nm. Unless specified otherwise, β-parinaric acid in ethanol was added to the dispersion in volume ~1 μl/ml resulting in a probe to lipid ratio of less than 1:100. 2, 6-di-tert-butyl-4-methylphenol (BHT), obtained from Nutritional Biochemicals, was added, in approximately equimolar ratio to the parinaric acid, as antioxidant.

Miscellaneous Materials

dl-Dipalmitoyl phosphatidylcholine (DPPC) was obtained from Sigma Chemical Co., and used without further purification. Commercial cholesterol was recrystallized from glacial acetic acid, washed with methanol, and dried (melting point 149°C). Bovine serum albumin (BSA), lyophilized and crystallized and essentially fatty acid-free was obtained from Sigma.

Spectroscopy

Absorption spectra were recorded on a Cary 14 scanning spectrophotometer. When peak positions were being determined, the spectra were recorded at the scan rate of 10 nm/2 min; the chart rate was set at 1 inch/min. The absorption maxima were estimated to the nearest 0.1 nm and repetitive determinations indicated that peak positions for parinaric acid could be reproducibly measured to ± 0.2 nm.

Fluorescence spectra were recorded on an Hitachi-Perkin-Elmer MPF-2A fluori-

meter attached to a Moseley 7030A X-Y recorder. In phase transition determinations, the sample temperature was monitored by a copper-constantan thermocouple inside a jacketed cuvette and the output of the thermocouple was used to drive the X axis of the recorder. The fluorimeter output, scaled by a Keithley-621 Electrometer was used to drive the Y axis.

Sample temperature was controlled in the jacketed cuvette by a circulating water bath. In fluorescence scans, the rate of temperature change never exceeded 2°/min. In absorption measurements, the temperature was allowed to equilibrate for 10 min. In lipid experiments, the sample cuvette was deoxygenated with argon, and the sample was always allowed to equilibrate at a temperature above the transition temperature of the lipid. Temperature scans were always decreasing then increasing in temperature, sometimes with multiple scans. The precautions taken (BHT and argon) were sufficient to insure against probe degradation and only small variations in fluorescence intensity at high and low temperature were observed from scan to scan.

RESULTS

Spectroscopy of Polyene Fatty Acids

Figure 1 shows the spectra of some linear polyenes in methanol at 25°C. α-Parinaric acid has absorption maxima at 303 nm ($\epsilon = 80 \times 10^3$) and 318 ($\epsilon = 74 \times 10^3$) and a broad emission maximum near 410 nm with quantum yield, Q, equal to 0.015 ± 0.005 (4). The emission spectrum originates from a state of lower energy and symmetry different from the state responsible for the strong absorption, a property which is characteristic of linear polyenes (5). As a result, absorption and emission are widely separated and are not mirror images. The all trans isomer, β-parinaric acid, has absorption maxima in methanol at 299 nm ($\epsilon = 91 \times 10^3$) and 313 nm ($\epsilon = 84 \times 10^3$) and emission properties similar to the cis species. The absorption spectrum of α-eleostearic acid (9, 11, 13-cis, trans, trans-octadecatrienoic acid) is also shown with its maximum (271 nm and $\epsilon \sim 48 \times 10^3$ [11]) and weak fluorescence maximum (near 345 nm, not shown) in the same spectral regions as the absorption and fluorescence of tryptophan. The absorption peak of β-parinaric acid in a bilayer lipid membrane ranges from about 317 to 321 nm and absorbs the radiation of commercial helium-cadmium lasers (325 nm).

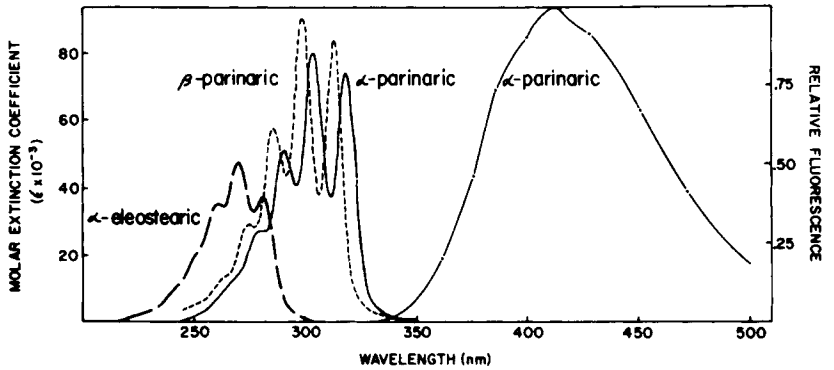

Fig. 1. Linear polyene spectra. The absorption spectra are shown for α-eleostearic acid (– –), α-parinaric acid (–), and β-parinaric acid (- - -). The fluorescence emission of α-parinaric acid (• – •), is shown as relative fluorescence, arbitrary units, scaled to 1.0 at the maximum at 410 nm (uncorrected spectrum). Excitation at 320 nm with slit width 3 nm and emission slit width 8 nm were used. Measurements were made in methanol at 25°C.

Tryptophan fluorescence from proteins depends upon the environment of the tryptophyl residues. The emission maximum generally lies between 330 and 350 nm (12, 13). The Förster equation (14) predicts energy transfer between tryptophan as donor and either α- or β-parinaric acid as acceptor due to spectral overlap between tryptophan fluorescence and parinaric acid absorption. The Förster equation is given by (15):

$$R_0 = \left(\frac{JK^2Q_0}{n^4}\right)^{1/6} (9.79 \times 10^3),$$

where R_0 = the distance (in Å) at which the transfer efficiency is 50%, K^2 = the orientation factor for dipole-dipole transfer, Q_0 = the quantum yield of the donor in the absence of transfer, n = refractive index of the medium, J = the spectral overlap integral (in $cm^3\ M^{-1}$), is given by

$$J = \frac{\int F(\lambda)\,\epsilon(\lambda)\,\lambda^4\,d\lambda}{\int F(\lambda)\,d\lambda},$$

where F (λ) and ε (λ) are the fluorescent intensity of the donor and extinction coefficient of the acceptor, respectively, at wavelength λ.

The spectral overlap, shown in Fig. 2 for α-parinaric acid, bound to BSA, with BSA tryptophan emission is calculated to be $\sim 125 \times 10^{-16}$ ($cm^3\ M^{-1}$). In calculating an approximate R_0, we use the following values: $Q_0 = 0.4$ is the experimental value determined for tryptophyl residues in BSA and is somewhat larger than the quantum yields which are determined for tryptophyl residues in other typical proteins (12). K^2 is assumed to equal 1, which represents an effective dipole orientation for transfer, and n is set equal to 1.4. The calculated value of R_0 is 30–35 Å.

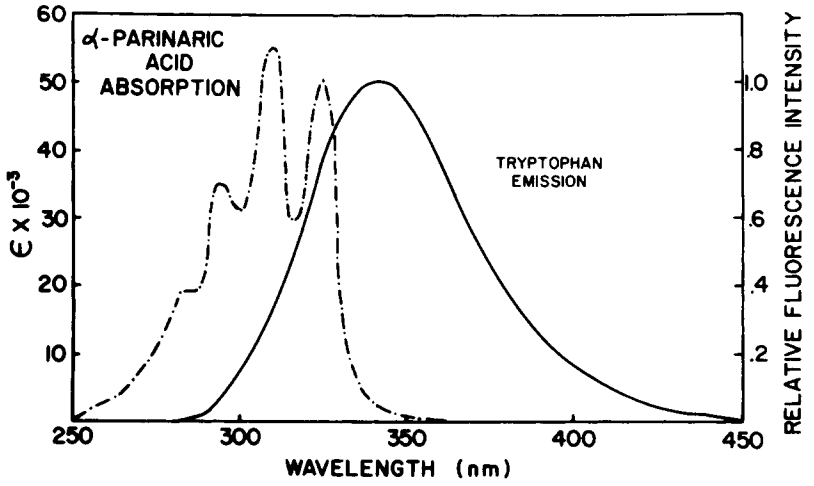

Fig. 2. Spectral overlap. The emission spectrum for tryptophyl residues (uncorrected) in BSA in a buffered aqueous solution containing 1.20 mg/ml was recorded using excitation at 260 nm (slit width 8 nm). The emission spectrum was scanned (slit width 2.5 nm) and shows a maximum near 342 nm. The absorption spectrum for α-parinaric acid was obtained under conditions where nearly complete binding to bovine serum albumin is observed (for example, see Fig. 7). The peak position at the first absorption maximum is ~324 nm at molar ratio 4 moles parinaric acid/mole BSA) and ϵ_{max} (309 nm) is $\sim 55 \times 10^3$.

Effect of Probe Concentration on the DPPC Phase Transition

We have previously demonstrated changes in fluorescence intensity of parinaric acid probes when synthetic phospholipids undergo thermal transitions (4). Figure 3 shows the effect of increasing the amount of free β-parinaric acid on the phase transition of an aqueous dispersion of dipalmitoyl phosphatidylcholine (DPPC). For the purpose of comparison, the fluorescence intensity in the samples has been adjusted to a height of 50 arbitrary fluorescence units at 30°C. With a lipid to probe ratio 1,000:1, the transition is 1° wide and shows a hysteresis of 1°. Both of these effects may be partially kinetic and result from the rate of temperature variation which was 2°/min. At a ratio of 100:1, the hysteresis and transition width are each ~2°C, but the relative intensity through the transition region is basically unchanged. At a ratio of 10:1, the transition has broadened to ~7.5°C, although neither the hysteresis nor the transition midpoint has varied significantly. In each of these cases, BHT (2, 6-di-tert-butyl-4-methyl phenol), a lipophilic antioxidant, has been added in the ratio 1 mole BHT: 1 mole parinaric acid. Experiments at lower concentrations of BHT (lipid to probe ratio, 10:1 and parinaric acid to BHT ratio 100:1) show a width of 5°C and hysteresis reduced to ~1.5°, indicating that some of the width and hysteresis is attributable to the BHT. We have noted that, in general, sonicated samples display wider transitions than are observed with dispersions prepared by mixing and a hysteresis that is typically less than 1°C. Similar transition curves are observed by using free α-parinaric acid or 2-parinaroyl, 1-palmitoyl phosphatidyl choline as probes (4). The fact that the adjusted intensity through the transition does not vary as a function of probe concentration indicates that the amount of probe in the lipid phase is similar above and below the transition. Taken together, these latter two facts indicate that the primary mechanism of the probes' responsiveness is due to changes in the lipid environment rather than to exclusion from the lipid phase as it melts. In contrast, 1-anilino-8-naphthalene sulfonate (ANS) binds more effectively to fluid than solid lipids (16). We have not yet determined the solubility limits of parinaric acid in lipid bilayers.

Results for Other Lipid Systems

When phase transition data is displayed as log fluorescence intensity vs. 1/T, the regions above and below the transition temperature give nearly straight lines (for example, see Fig. 5) with slopes which appear to be characteristic of the probe used and of the lipid (4).

Preliminary results for a binary phase diagram of the mixture DPPC with dipalmitoyl phosphatidylethanolamine (DPPE) determined with β-parinaric acid are nearly identical to that determined by other methods (17), indicating that this probe will be useful in studying lateral phase separations in complex mixtures, including biological membranes.

When α-parinaric acid (cis, trans, trans, cis) is added to a mixture containing dimyristoyl phosphatidylcholine (DMPC) vesicles and distearoyl phosphatidylcholine (DSPC) vesicles, distinct transitions for both of the lipids are observed by fluoresence. Repetitive scans show both transitions, indicating that α-parinaric acid remains distributed between fluid and solid lipids. On the other hand, when β-parinaric acid (all trans) is added to a similar mixture, only the higher temperature DSPC transition is detected. When β-parinaric acid is added to DMPC alone (in which the phase transition is detected) and then DSPC vesicles are added, subsequent scans show only the DSPC transition. It appears that β-parinaric acid is excluded from the DMPC vesicles at 24°C as the DMPC undergoes thermal transition to the fluid state and, from that time on, only DSPC transitions are

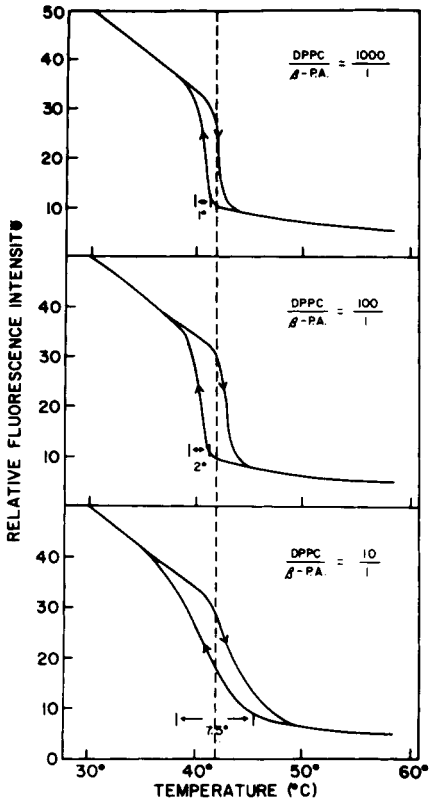

Fig. 3. Effect of probe concentration on DPPC phase transition. Dispersions of DPPC in 40 ml of 0.066 M potassium phosphate buffer, pH 6.7, prepared in the concentrations 2.1×10^{-5} M (0.016 mg/ml), 4.2×10^{-5} M (0.032 mg/ml), and 2.1×10^{-4} M (0.16 mg/ml). β-Parinaric acid solutions in ethanol (~0.5 mg/ml were added to the dispersion in the amounts 50 μl, 10μl, and 5 μl to produce solutions which had lipid to probe ratios of approximately 10/1, 100/1, and 1,000/1, respectively. BHT in ethanol was added in approximately equimolar ratio to the parinaric acid. The solutions were then deoxygenated with argon, warmed to 50°C, and vortexed. Fluorescence measurements were carried out using excitation wavelength 321 nm (with slit width 1.5 nm) and emission at 410 nm (with slit adjusted from sample to sample to compensate for varying probe concentration). The sample was cooled from 60°C at the rate of 2°C/min, then heated from 25°C at the same rate.

detected. This differential partitioning, probably related to the different molecular shapes of the two probes, may prove useful in studying processes in distinct phases of complex lipid systems with laterally separated components.

Preliminary measurements indicate that polarization of fluorescence provides a means of studying the motional freedom of the probe molecule in its lipid environment. We have measured the ratio of fluorescence intensity parallel ($I_{||}$) and perpendicular ($I_{\perp}$) to a polarized exciting beam. β-parinaric acid, in DPPC below its phase transition temperature, has $I_{||}/I_{\perp}$ equal to 2.5–2.8. Above the transition, the ratio equals 1.4–1.6. In the transition region the ratio varies rapidly between these limits. The limits correspond to the probe nearly rigidly fixed in the solid phase and mobile in the fluid phase.

When Ca^{++} is added to a dispersion of neutral phospholipids (DPPC or DPPE) several parameters of the phase transition measured by ANS are affected (16). In contrast, we can, using β-parinaric acid as probe, detect no changes either in magnitude, width, or

hysteresis up to 10 mM Ca^{++}. In these experiments, the lipid (0.05 mg/ml, 6×10^{-2} mM) was dispersed by vortexing in N-2-hydroxyethylpiperazine-N'-2-ethanesulfonic acid (HEPES) buffer (0.01 M), pH 7.0

DPPC/Cholesterol Studies

Figure 4 shows the determination of a phase transition in DPPC and cholesterol/DPPC dispersions by wavelength shift of the β-parinaric acid absorption peak position, and Fig. 5 shows a fluorescence measurement on the same samples upon completion of the absorption measurements. The feasibility of the absorption shift method was determined by comparing the lipid results with wavelength positions for β-parinaric acid in decane vs. temperature, where no point lies off the line shown by more than 0.2 nm. Although the total shifts are small (~2 nm through the transition for pure DPPC and ~1 nm for a 3:10 molar ratio of cholesterol/DPPC) in the lipids, no point or duplicate in a

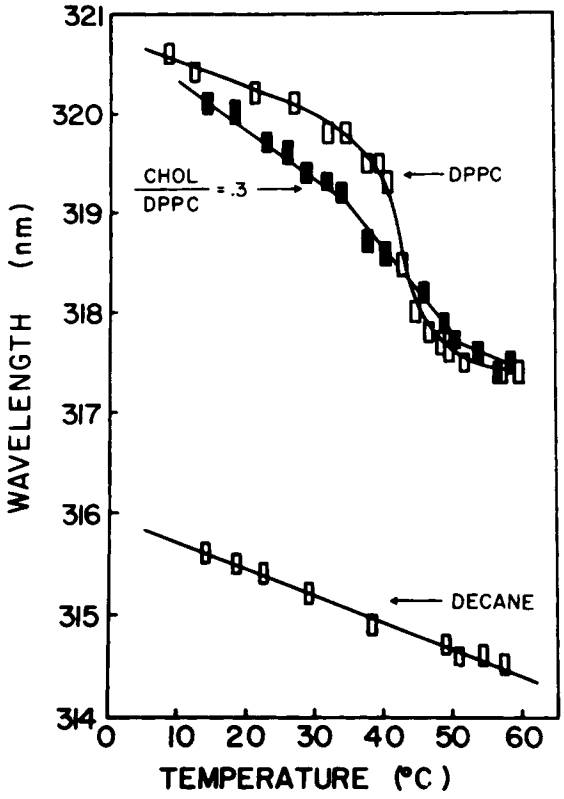

Fig. 4. Determination of phase transitions by shifts in absorption peak position. Two lipid dispersions were prepared by brief sonication (30 sec, 50 W) under argon in pH 7.5, 0.01 M phosphate buffer. The first contained DPPC (0.10 mg/ml, 1.3×10^{-4} M and the second contained DPPC (1.0×10^{-4} M, 0.075 mg/ml), and cholesterol (0.30×10^{-4} M, 0.012 mg/ml). 5 μl of an ethanolic solution of β-parinaric acid (~0.6 mg/ml) was added to 2 ml of each dispersion, resulting in solutions which were 6×10^{-6} M in probe. In each case the lipid to probe ratio was ~20/1. BHT was added in equimolar ratio to the probe. The samples, deoxygenated with argon, were referenced vs. identical temperature-controlled cuvettes containing the lipid dispersion with BHT, but no probe, to correct for any absorption changes that might result from changes in the light-scattering properties of the lipid dispersions as they undergo phase transitions. The data for parinaric acid in decane (no lipid present) were obtained in similar fashion.

series of decreasing and then increasing temperature points, obtained at equilibrium, varies by more than 0.2 nm from the lines drawn. These dispersions were sonicated briefly to obtain clear solutions for measuring absorption changes.

Fluorescence studies in both sonicated (using the phospholipid probe) and unsonicated dispersions over a range of cholesterol concentrations give essentially the same results. As cholesterol is increased, the transition diminishes and broadens, without significant change in the transition midpoint temperature. These preliminary studies show that the transition disappears at 1:1 molar ratio cholesterol/DPPC. The results are consistent with the notion that cholesterol orders the fluid phase and disorders the solid phase (18, 19), since neither the fluorescence nor the peak position at high or low temperature limits achieves the levels in cholesterol/DPPC mixtures that they do in pure DPPC. Our results do not distinguish between lateral phase separation of the components of lecithin-cholesterol mixtures (20) or the more specific hypothesis of the formation of equimolar complexes (21).

Interpretation of Spectral Changes

The shift in the parinaric acid absorption spectrum on either side of the membrane phase transition can be explained in terms of simple theories of solvent shifts for electronic spectra (22–24). Application of these simple theories to linear polyene spectra has shown that the strong transition, i.e. the absorption, of these nonpolar chromophores shifts

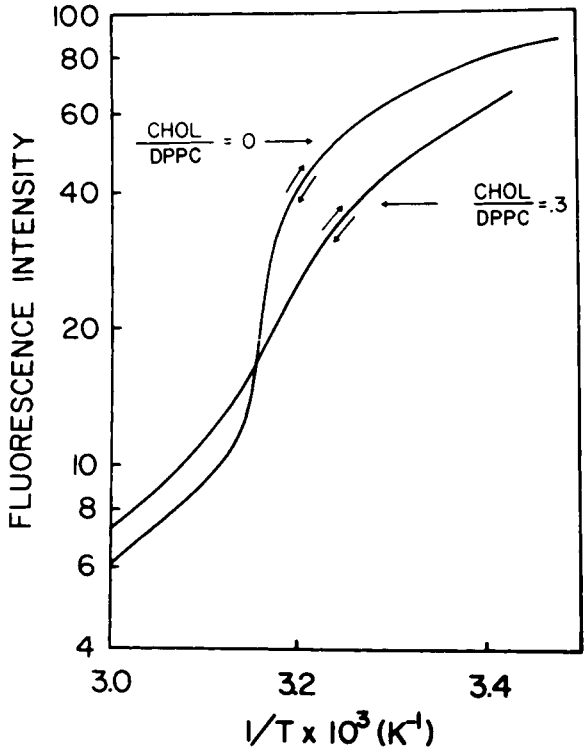

Fig. 5. DPPC and DPPC/cholesterol. Upon completion of the measurements described in Fig. 4, phase transitions for the samples were measured by fluorescence as described in Materials and Methods. Identical conditions were used for each with excitation at 318 nm (slit 1.5 nm) and emission at 420 nm (slit 14 nm).

primarily in response to the polarizability of the environment and little or not at all in response to the solvent polarity (5). This situation arises in part because neither the ground nor the excited states of linear polyenes has a dipole moment and because the polyene electronic transition dipole is very large. The polarizability of the solvent, α_s, is a measure of the response of the solvent electron clouds to the high frequency transient dipole induced by an electronic transition. It is related to the refractive index of the medium by

$$\alpha_s = \frac{n^2 - 1}{n^2 + 2},$$

or similar expressions (22–24). The refractive index should be that measured for the solvent near the frequency of the electronic transition. Theory and experiments on other polyenes (5) and parinaric acid have established a relationship between the solvent polarizability, α_s, and the spectral transition of the form

$$\bar{\nu} = \bar{\nu}^0 - k\alpha_s,$$

where $\bar{\nu} = 1/\lambda$, $\bar{\nu}^0$ refers to the gas phase, and k is a constant on the order of 10,000 cm^{-1}. The bilayer lipid membrane presents an anisotropic polarizability to the polyene probe and the mean polarizability reflected in the spectral shift is, in principle, a function of both the membrane structure and the polyene transition dipole orientation. If the lipid bilayer is assumed to have an isotropic polarizability then the observed wavelength shift can be interpreted as resulting from a 10% expansion of the bilayer through the phase transition.

The strongly allowed electronic transition of linear polyenes is not the lowest energy transition, and the excited state produced by this transition is not the state from which fluorescence originates (5). Polyenes have a weak transition below the strongly allowed transition whose intensity is primarily borrowed from the allowed transition by vibronic mixing and other molecular distortions. The net result is that the intrinsic fluorescence lifetime for a polyene, τ_O, is much longer than expected on the basis of its integrated (strong) absorption spectrum and τ_O depends on the solvent polarizability. This is because the intensity borrowed from the strong transition depends on the energy difference between the excited states (as ΔE^{-2}), and this energy difference is a function of solvent polarizability via differential solvent shifts of the form discussed above. The fluorescence quantum yield, Q, is given by

$$Q = k^0 / (k^0 + k_{nr}),$$

where $k^0 = 1/\tau^0$ is the radiative rate constant, and k_{nr} is the sum of all first-order non-radiative decay rates. We are therefore able to construct a relationship between Q and the solvent polarizability-containing constants evaluated from independent experiments. However, k_{nr} is also a function of the solvent and the temperature for reasons which are not yet certain but which probably involve the conformational and vibrational flexibility of the probe in its environment. Further work on the nature of the variation of Q with environment will involve lifetime measurements so that k^0 and k_{nr} can be separated.

A plot of log fluorescence intensity of parinaric acid vs. 1/T for various solvents is a straight line with characteristic slope depending upon solvent (not shown). Likewise in a lipid dispersion the high temperature (fluid phase) region and low temperature (solid phase) region are nearly linear plots of log fluorescence intensity vs. 1/T with slope characteristic of the phase. We view the change in fluorescence quantum yield with

temperature as being due in part to the variation of the energy difference between the excited states and the resulting variation in the intrinsic transition probability for the fluorescence. The excited state energy spacing varies with temperature because the thermal expansion of the solvent moves the absorption to higher energy due to a decreasing α_s. Some of the variation of Q with T is probably due to a variation in radiationless decay rate, k_{nr}, rather than the radiative rate k^0. Measurements on other polyenes have shown that k^0 does in fact change with temperature in a manner consistent with our model (25).

Since the fluorescence involves a symmetry-forbidden transition originating from an excited state that is only slightly lower in energy than the state involved in the strong absorption spectrum (5), the fluorescence of linear polyenes is particularly sensitive to environmental perturbations. The two low energy excited states can be mixed by conformational distortions and static electric fields, resulting in changes in fluorescence quantum yield.

Lipid-Protein Interactions

The activity of some membrane-bound proteins is modulated in part by lipid organization, at least with respect to thermal phase transitions of a single component or lateral phase separations in a multi-component membrane (26). It is our intention to use the spectral properties of parinaric acid to monitor lipid-protein interactions. To this purpose we have chosen, as a model, bovine serum albumin (BSA), a well-characterized protein with binding sites for free fatty acids which is obtainable commercially electrophoretically pure.

Previously, detailed binding studies with human serum albumin for a variety of fatty acids (27) and bovine serum albumin have been carried out (28, 29). Bovine serum albumin has two tryptophyl residues, both of which are exposed to the aqueous phase (12); one lies near a site of high binding affinity for fatty acids (28, 30). We have explored the binding of α-parinaric acid to bovine serum albumin through four spectroscopic techniques.

α-Parinaric acid bound to bovine serum albumin has its fluorescence quantum yield enhanced 50-fold over its aqueous value. One study (not shown), carried out at constant α-parinaric concentration and varying BSA concentrations, is amenable to Scatchard analysis and indicates a total of five to six binding sites with a $K_B \approx 10^7$ (M^{-1}) for the last three to four binding sites. Approximately two other sites have indeterminate but higher K_B by this method.

Figure 6 shows the binding of varying amounts of α-parinaric acid to BSA. The open circles show the quenching of tryptophan fluorescence by energy transfer to bound parinaric acid. A line tangent to the initial section of this curve extrapolates to 50% quenching at ~1 mole parinaric acid/mole BSA. Since the two tryptophyl residues have similar quantum yields (12), it can be suggested that the 1st mole of parinaric acid added binds to the highest affinity binding site and completely quenches a nearby tryptophyl residue. We believe this site can hold two parinaric acid molecules. The filled circles show the fluorescence of parinaric acid upon binding. A line tangent to the initial segment of this curve extrapolates to a value close to 5 moles parinaric acid/mole BSA.

The shift of parinaric acid peak absorption position as a function of the polarizability of the environment can also be used to advantage. Figure 7 shows a binding study carried out by measuring the parinaric acid absorption peak position as a function of the ratio of α-parinaric acid to BSA. The filled rectangles show the peak position of the 1st absorption maximum of parinaric acid added to a solution containing BSA; each point represents the

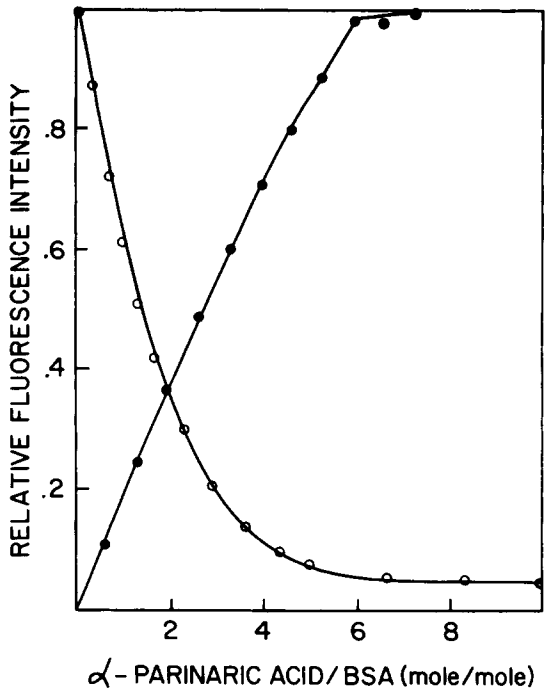

Fig. 6. Binding of α-parinaric acid to bovine serum albumin. Open circles (○—○) show the quenching of tryptophan fluorescence with increasing amounts of α-parinaric acid. To 25 ml of 0.01 M phosphate buffer, pH 7.4, containing 2.42 mg of BSA (3.50×10^{-8} moles), were added aliquots of α-parinaric acid in ethanol (2.32×10^{-9} moles/μl). Excitation of 230 nm (slit width 10 nm) avoids direct excitation of parinaric acid; the emission maximum was near 342 nm (slit width 10 nm). The contribution of tyrosine emission at 342 nm was judged to be small. Direct absorption of tryptophan emission at 342 nm by parinaric acid was minimal. Closed circles (●—●) show the emission of α-parinaric acid bound to BSA. To 25 ml of 0.01 M phosphate buffer, pH 7.4, containing 1.21 mg BSA (1.75×10^{-8} moles), were added aliquots of α-parinaric acid in ethanol (2.32×10^{-9} moles/μl). The excitation wavelength at 328 nm (slit width 3 nm) and emission maximum near 410 nm (slit width 10 nm) avoids substantial fluorescence from tryptophan. Results have been corrected for the absorption of exciting light by increasing amounts of parinaric acid. In both cases, the solutions were allowed to equilibrate for 10 min at 26°C after aliquot addition; the experiments were carried out below the total solubility limits of α-parinaric acid and the presence of small amounts of ethanol (ca. 0.4% by volume) were judged to have minimal perturbing effects. The fluorescence of free parinaric acid in buffer is less than 2% of bound parinaric acid.

mean of two independent measurements on separate samples in which no value varied by more than 0.2 nm. The peak position does not shift until ~2 moles parinaric acid have been added. The observed shift is to longer wavelength in contrast to the expected shift toward shorter wavelength if the additional fatty acid were dissolved partially in the aqueous environment (with limiting value 320.8 nm). The maximum wavelength position is between 5 and 6 moles added, and then the position moves to shorter wavelengths as the binding sites (five to six total, as determined by fluorescence) are saturated and the additional moles of fatty acid are added to the aqueous phase.

The difference spectra (open rectangles) represent the peak position in samples with n moles fatty acid to 1 mole BSA vs. reference samples containing n-1 moles fatty acid to 1 mole BSA. The difference spectra give information of the distribution of the nth mole

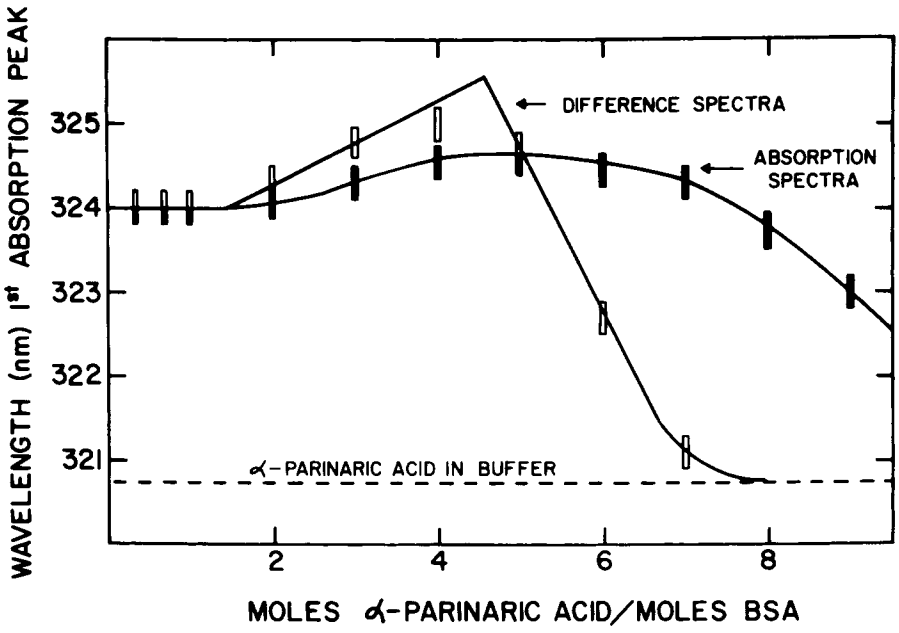

Fig. 7. Binding of α-parinaric acid to bovine serum albumin by absorption spectroscopy. Three 4.0-ml solutions, in standard 1-cm path quartz cuvettes, pH 7.4, 0.01 M potassium phosphate at room temperature contained 0.200 mg/ml BSA, resulting in concentrations of BSA 2.9×10^{-6} M. Aliquots of a standard parinaric acid solution were added to samples 1 and 2. (A 5-μl aliquot, the size generally added, gives a solution which has a molar ratio of parinaric acid to BSA nearly equal to 1/1.) Sample 3 was used as a reference, and aliquots added to it contained only ethanol. To construct the curve of the peak positions of absorption spectra as shown by the filled rectangles, sequential aliquots of parinaric acid were added to samples 1 and 2 at intervals of approximately 1 hr. The peak positions in samples 1 and 2 were measured against reference solution 3. To construct the difference spectra peak position curve, the peak positions in difference spectra of sample 1 (after n aliquots) vs. sample 2 as reference (after n-1 aliquots) were measured. Under these conditions, a difference spectra represents the binding distribution of the last added mole of parinaric acid and provides a $\Delta OD_{325\ nm} \sim 0.15$.

of fatty acid added and reduces some of the measurement errors associated with the small spectral shifts. The 1st mole (peak 324.0 nm) is entirely bound by a class of binding sites of high affinity. The 2nd mole is distributed between the first class and a second class of weaker affinity. The first class has approximately two sites, so the 3rd mole saturates the first class and is distributed between the second class and the aqueous phase. The 4th through 7th moles are partitioned between the second class and increasingly to the aqueous phase. The extinction coefficients in these three environments are similar ($\sim 60 \times 10^3$). If it is assumed that the peak position is a linear combination of the peak positions of the three species (distributed between the three distinct environments), then the total number of binding sites and binding constants for each class of sites can be estimated. We have assumed that binding to the second class of sites results in a peak position of 325.5 nm, the intersection shown in Fig. 7. These measurements have been repeated for the second peak position of parinaric acid, and independently for difference spectra where the sample containing n moles parinaric acid was compared to a reference containing n-2 moles parinaric acid. The plots are all quantitatively similar and peak positions agree in all cases to within 0.2 nm. The difference spectra at $n \geqslant 8$ gives peak positions consistent

with distribution of these last added moles of fatty acid entirely in the aqueous phase. Taken together, our results are consistent with the measurements by Goodman for the binding of oleic acid to human serum albumin. We conclude that two sites have binding constant $K_B \sim 10^8$ (M^{-1}) and three to four sites have binding constant $K_B \sim 10^6$–10^7 (M^{-1}). We cannot rule out multiple stepwise equilibria (29). However these classes of sites appear to be spectrally distinct.

We have also observed (4) a strong and complex induced circular dichroism ($[\theta]_{max} \sim 40 \times 10^3$) of the polyene bound to bovine serum albumin. Interpretation and application of this effect will be discussed elsewhere. There is also evidence that parinaric acid has somewhat different fluorescence quantum yields in the two classes of sites. These results combined with the spectral shifts just mentioned, the differential quenching of tryptophan fluorescence, and expected fluorescence lifetime differences for parinaric acid in different sites permit fairly complete characterization of the lipid-binding sites of BSA. Competition experiments can be performed in order to determine the affinity of other fatty acids for the BSA binding sites. This variety of spectral methods makes parinaric acid a general probe of lipid binding to proteins which should be applicable to membrane-bound proteins as well as to those free in solution.

E. Coli Phase Transition

The unsaturated fatty acid auxotroph of E. coli, 30E βox^- (26), will biosynthetically incorporate small amounts of parinaric acid while utilizing oleic acid or elaidic acid as a growth supplement. When the cell phospholipids contain substantial amounts of either oleic or elaidic acid, phase transitions, as shown in Fig. 8, are detected in intact cells and the extracted phospholipids. Comparable transitions are observed in control cells to which small amounts of β-parinaric acid have been added after the completion of growth (not shown). The transition results are in agreement with those reported by other techniques (3, 26).

CONCLUSIONS

The conjugated tetraene fatty acid, parinaric acid, has been found to be a useful probe for studying lipid-lipid and lipid-protein interactions. Three forms of this probe have been prepared and characterized: two geometrical isomers of the free fatty acid and synthetic phospholipids containing the polyene in the β-position.

Fluorescence and absorption measurements as a function of temperature have shown that these probes can be used to monitor the phase transition of bilayer lipid membranes. Cholesterol addition to DPPC dispersions broadens the transition and decreases its magnitude. In addition, phase diagrams of binary component systems can be constructed, the effects of cations on transitions can be studied, and probe mobility in solid or fluid phospholipids can be studied by fluorescence depolarization. The probe in the bilayer responds to changes in the polarizability of the hydrocarbon as the chains melt, and, in contrast to the well-known fluorescent probe ANS, the magnitude of the transition does not appear to be affected by the concentration of the probe or the presence of Ca^{++}.

Lipid-protein interactions can be monitored with parinaric acid by a variety of spectral measurements including absorption shifts, fluorescence quantum yield increases, tryptophan fluorescence quenching, and induced circular dichroism. This variety of measurements means that different classes of binding sites may be distinguished spectrally

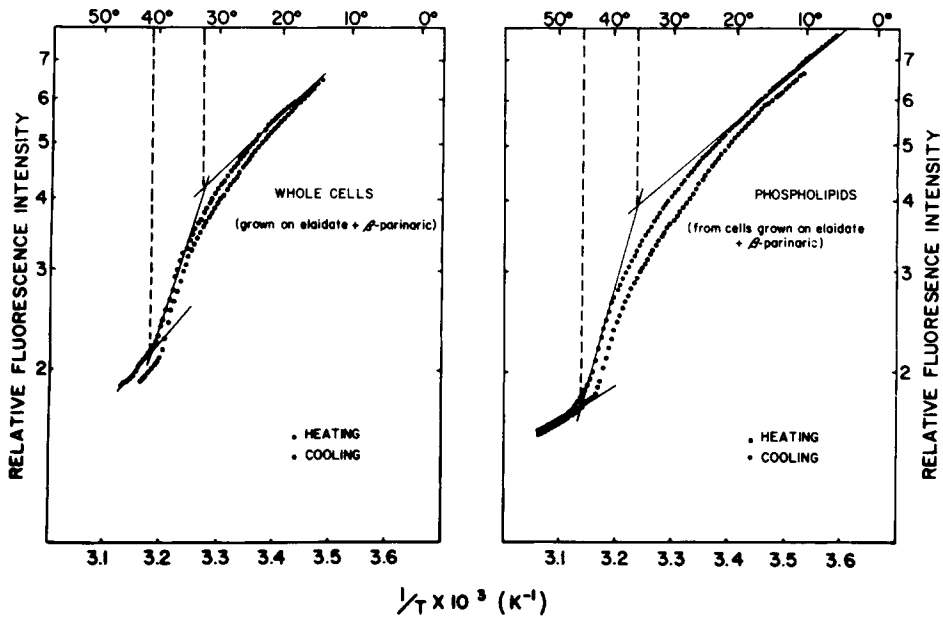

Fig. 8. Determination of thermal phase transitions for E. coli cells and phospholipids. E. coli strain 30E βox^- were grown in the presence of β-parinaric acid (20 μg/ml) and elaidic acid (20 μg/ml) as a growth supplement at 40°C, as previously described (26). Late log-phase cultures were harvested and washed and cells were resuspended to ~5 X 10^{10} cells/ml in salts solution. They were then further diluted 50-fold in salts solution giving a suspension suitable for fluorimetry. Typically, excitation at 320 nm (slit 2 nm) and emission at 500 nm (slit 40 nm) were used to minimize contributions of other fluorescing cellular components. Temperature variation was at the rate of 1°C/min, beginning at high temperature, decreasing to ~5°C, then reversing direction. Phospholipids, extracted and chromatographically purified, contained ~0.1% esterified β-parinaric acid. These phospholipids, dispersed (~0.05 mg/ml) in buffer, showed similar transitions using excitation at 320 nm (slit 2 nm) and emission at 410 nm (slit 40 nm), since no adjustment is needed for cellular fluorescence. The data are displayed as log fluorescence intensity vs. 1/T (K^{-1}). The tangents drawn suggest linear portions of the curves and the intersects may represent temperature values for the onset and completion of the transitions.

as well as on the basis of their binding constant. Studies with bovine serum albumin give results that are similar to those previously published using other techniques and serve as the basis for extending these studies to membrane proteins.

The electronic structure of linear polyenes has been the subject of recent high resolution, low temperature studies, fluorescence lifetime measurements, and theoretical investigations (5). The newly established order of excited states for polyenes indicates that the fluorescence of these molecules should be quite sensitive to environmental perturbations, including static electric fields.

The biosynthetic incorporation of parinaric acid into a fatty acid auxotroph of E. coli has been accomplished. Phase transitions detected in cells are similar whether the probe is biosynthetically incorporated or added to the cells after the growth is complete. These results substantiate the expectation that these probes exert a minimal perturbation of the biological membrane.

NOTE ADDED IN PROOF

More recent experiments have shown that the hysteresis observed in phase transitions (see Fig. 3) is related to the rate of change of temperature in the sample. When the temperature is varied at less than 0.5°C/min, the hysteresis becomes vanishingly small. The width of the transition is not strongly affected by the rate of temperature change.

Recent fluorescence lifetime studies indicate that polarizability changes account for only a small part of the observed variation in fluorescence intensity. The radiationless decay constant, k_{nr}, has been found to be strongly temperature dependent while the radiative rate constant, k°, remains nearly constant both as a function of temperature and environmental polarizability.

ACKNOWLEDGMENTS

We thank Mr. D. Koroveibau of the Department of Agriculture, Fiji, for kindly providing us with seeds of the plant Parinari glaberrima from which α-parinaric acid was isolated. We thank Mr. Stuart Bursten and Ms. Evelyn Tecoma for allowing us to use Figs. 3 and 8, respectively, Ms. Marianne Petersen for her skillful preparation and characterization of β-parinaric acid, and Drs. C. Linden and C. F. Fox for kindly providing the E. coli strain 30E βox . We gratefully acknowledge helpful discussions with Prof. E. Dratz and his suggestion of BHT as an antioxidant. This work was supported by National Institutes of Health Research Grants GM 21149 (to Bruce S. Hudson) and GM 18539 (to Robert D. Simoni). Bruce S. Hudson is an Alfred P. Sloan Fellow and Camille and Henry Dreyfus Teacher-Scholar.

REFERENCES

1. Radda, G. K., in "Current Topics in Bioenergetics," D. R. Sanadi (Ed.). Academic Press, New York and London. p. 81 (1971).
2. Waggoner, A. S., and Stryer, L., Proc. Natl. Acad. Sci. U.S.A. 67:579 (1970).
3. Träuble, H., and Overath, P., Biochim. Biophys. Acta 307:491 (1973).
4. Sklar, L. A., Hudson, B. S., and Simoni, R. D., Proc. Natl. Acad. Sci. U.S.A. 72, p. 1649 (1975).
5. Hudson, B., and Kohler, B., Annu. Rev. Phys. Chem. 25:437 (1974).
6. Riley, J. P., J. Chem. Soc. 12–18 1950: .
7. Kaufman, J. P., and Sud, R. K., Chem. Ber. 92:2797 (1959).
8. Gunstone, F. D., and Subbarao, R., Chem. Phys. Lipids 1:349 (1967).
9. Shinitzky, M. S., and Inbar, M., J. Mol. Biol. 85:603 (1974).
10. De Kruijff, B., Gerristen, W. J., Oerlemans, A., Demel, R. A., and Van Deenan, L. L. M., Biochim. Biophys. Acta 339:30 (1974).
11. Beilstein's Handbook, Vol. 2, Suppl. 2, p. 465 (1942).
12. Burstein, E. A., Vedenkina, N. S., and Ivkova, M. N., Photochem. Photobiol. 18:263 (1973).
13. Longworth, J. W., in "Excited States of Proteins and Nucleic Acids," R. F. Steiner and I. Weinryb (Eds.). Plenum Press, New York and London, pp. 432–433 (1971).
14. Forster, Th., in "Modern Quantum Chemistry," Istanbul Lectures. O. Sinanoglu (Ed.). Academic Press, New York. Section III-B, pp. 93 (1965).
15. Wu, C. W., and Stryer, L., Proc. Nat. Acad. Sci. U.S.A. 69:1104 (1972).
16. Träuble, H., Die Naturwissenschaften, 58:277 (1971).
17. Shimshick, E. J., and McConnell, H. M., Biochemistry 12:2351 (1973).
18. Ladbrooke, B. D., Williams, R. M., and Chapman, D., Biochim. Biophys. Acta 150:333 (1968).
19. Ladbrooke, B. D., and Chapman, D., Chem. Phys. Lipids 3:304 (1969).
20. Phillips, M. C., and Finer, E. G., Biochem. Biophys. Acta 356:199 (1974).
21. Shimshick, E. J., and McConnell, H. M., Biochem. Biophys. Res. Commun. 53:446 (1973).
22. Basu, S., Adv. Quantum Chem. 1:145 (1964).

23. Longuet-Higgins, H. C., and Pople, J. A., J. Chem. Phys. 27:192 (1957).
24. Ooshika, Y., J. Phys. Soc. Jap. 9:594 (1954).
25. Dalle, J. P., and Rosenberg, B., Photochem. Photobiol. 12:151 (1970).
26. Linden, C. D., Wright, K. L., McConnell, H. M., and Fox, C. F., Proc. Natl. Acad. Sci. 70:2271 (1973).
27. Goodman, D. S., J. Am. Chem. Soc. 80:3892 (1958).
28. Wallach, D. F. H., Verma, S. P., Wiedekamm, E., and Bieri, V., Biochim. Biophys. Acta 356:68 (1974).
29. Ashbrooke, J. D., Spector, A. A., Santos, E. C., and Fletcher, J. E., J. Biol. Chem. 250:2333 (1975).
30. Swaney, J. B., and Klotz, I. M., Biochemistry 9:2570 (1970).